Northrop, D. B. (1977) in *Isotope Effects in Enzyme-Catalyzed Reactions* (Cleland, W. W., O'Leary, M. H., & Northrop, D. B., Eds.) University Press, Baltimore, MD.
Northrop, D. B. (1982) *Methods Enzymol. 87*, 607.
Olson, J. S., Ballou, D. P., Palmer, G., & Massey, V. (1974a) *J. Biol. Chem. 249*, 4350.
Olson, J. S., Ballou, D. P., Palmer, G., & Massey, V. (1974b) *J. Biol. Chem. 249*, 4363.
Palmer, G., Bray, R. C., & Beinert, H. (1964) *J. Biol. Chem. 239*, 2657.
Palcic, M. M., & Klinman, J. P. (1983) *Biochemistry 22*, 5957.
Porras, A. G., Olson, J. S., & Palmer, G. (1981) *J. Biol. Chem. 256*, 9096.
Rajagopalan, K. V., & Handler, P. (1967) *J. Biol. Chem. 242*, 4097.
Saunders, W. H., Jr. (1985) *J. Am. Chem. Soc. 107*, 164.
Schopfer, L. M., Massey, V., & Nishino, T. (1988) *J. Biol. Chem. 263*, 13528.
Shore, J. D., & Gutfreund, H. (1970) *Biochemistry 9*, 4655.
Simon, H., & Palm, D. (1966) *Angew. Chem., Int. Ed. Engl. 5*, 920.
Waud & Rajagopalan, K. V. (1976) *Arch. Biochem. Biophys. 172*, 365.

Phosphorescence and Optically Detected Magnetic Resonance Studies of Echinomycin–DNA Complexes†

Thomas V. Alfredson and August H. Maki*
Chemistry Department, University of California, Davis, California 95616
Received March 15, 1990; Revised Manuscript Received June 22, 1990

ABSTRACT: Echinomycin complexes with polymeric DNAs and model duplex oligonucleotides have been studied by low-temperature phosphorescence and optical detection of triplet-state magnetic resonance (ODMR) spectroscopy, with the quinoxaline chromophores of the drug used as intrinsic probes. Although not optically resolved, plots of ODMR transition frequencies versus monitored wavelength revealed heterogeneity in the phosphorescence emission of echinomycin, which was ascribed to the presence of two distinct quinoxaline triplet-state environments (referred to as the blue and red triplet states of echinomycin in this report). We think that a likely origin of the two triplet states of echinomycin is the occurrence of two or more distinct conformations of the drug in aqueous solutions. Spectroscopically observed perturbations of the triplet-state properties of echinomycin such as the phosphorescence emission spectrum, phosphorescence lifetime, ODMR spectrum, and zero-field splitting (zfs) energies were investigated upon drug binding to the double-stranded alternating copolymers poly(dG-dC)·poly(dG-dC) [abbreviated as poly[d(G-C)$_2$]] and poly(dA-dT)·poly(dA-dT) [abbreviated as poly[d(A-T)$_2$]], the homopolymer duplexes poly(dG)·poly(dC) [abbreviated as poly(dG·dC)] and poly(dA)·poly(dT) [abbreviated as poly(dA·dT)], and the natural DNAs from *Escherichia coli*, *Micrococcus lysodeikticus*, and calf thymus. Echinomycin bisintercalation complexes with the self-complementary oligonucleotides d(ACGT), d(CGTACG), and d(ACGTACGT), which are thought to model drug binding sites, were also investigated. Phosphorescence and ODMR spectroscopic results indicate that the quinoxaline chromophores of the drug are involved in aromatic stacking interactions in complexes with the natural DNAs as evidenced by red shifts in the phosphorescence 0,0 band of the drug, a small but significant reduction in the phosphorescence lifetime of the red triplet state, and reduction of the zfs *D*-value of both the blue and red triplet states upon drug complexation. These changes in the triplet-state properties of echinomycin are consistent with stacking interactions that increase the polarizability of the quinoxaline environment. The extent of the reduction of the *D* parameter for the red triplet state upon complexation with the polymeric DNAs was found to correlate with the binding affinities measured for these targets [Wakelin, L. P. G., & Waring, M. J. (1976) *Biochem. J. 157*, 721–740], with the single exception of the drug–poly[d(G-C)$_2$] complex, for which an increase in the *D*-value was noted. In addition, upon drug binding to the natural DNAs, there is a reversal of signal polarity in the ODMR spectra of the red triplet state. Among the synthetic DNA polymers investigated, a reversal of ODMR signal polarity was found only with the echinomycin–poly[d(A-T)$_2$] complex. The polarity reversals apparently result from changes in the triplet sublevel decay constants upon binding to DNA. Echinomycin binding to the duplex oligonucleotides employed in this work gave results similar to those obtained with the natural DNAs. In relation to the other DNA complexes, the echinomycin–d(CGTACG) complex exhibited significantly enhanced ODMR signals for a blue-shifted triplet state, which were ascribed to solvent-exposed quinoxaline rings at either end of the oligonucleotide lattice as deduced from X-ray diffraction studies [Ughetto, G., et al. (1985) *Nucleic Acids Res. 13*, 2305–2323].

Quinoxaline antitumor antibiotics, the natural products of several species of *Streptomycetes*, are composed of two planar quinoxaline-2-carboxamide moieties linked by a cross-bridged, cyclic octadepsipeptide. Two families of quinoxaline antibiotics are known, the triostins and the quinomycins, that differ in their respective cross-bridge structure. Echinomycin (Figure 1) is the most prominent member of the quinomycins, which contain a thioacetal cross-linkage. Its biological activity as

† This research was partially supported by NIH Grant ES-02662 and by a grant from the University of California, Davis, Committee on Research.

0006-2960/90/0429-9052$02.50/0

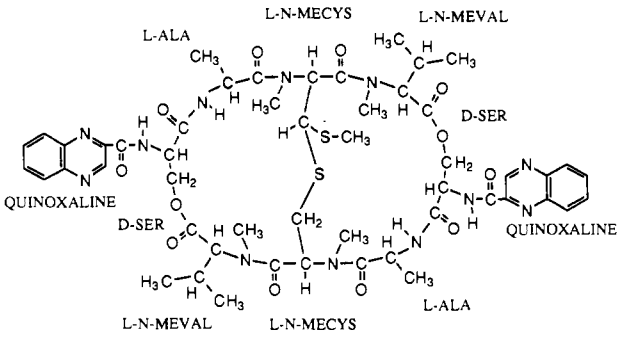

FIGURE 1: Structure of echinomycin.

an antitumor agent has been attributed to DNA[1] binding, which selectively inhibits both DNA replication and DNA-directed RNA synthesis (Ward et al., 1965; Sato et al., 1967).

Early investigations of echinomycin complexation to circular DNA and sonicated rodlike DNA fragments (Waring & Wakelin, 1974; Wakelin & Waring, 1976) proposed a bisintercalation mode of binding on the basis of helix extension and helix-unwinding angles relative to ethidium. Recent single-crystal diffraction studies of the echinomycin–d(CGTACG) complex and the related triostin A complex (Wang et al., 1984; Ughetto et al., 1985) as well as NMR solution studies of echinomycin complexes with d(ACGT) and d(TCGA) tetramers (Gao & Patel, 1988) and the DNA octamer d(ACGTACGT) (Gilbert et al., 1989) have corroborated the bisintercalation binding mode. Echinomycin was shown to bisintercalate into the minor groove of the double helix where the quinoxaline chromophores sandwich a CpG base sequence. Hydrogen bonding of the alanine residues with guanine bases, numerous van der Waals contacts between the peptide and the nucleic acid target, and stacking interactions between the quinoxaline rings and the nucleic acid bases were found to contribute to stabilization of the drug–DNA complexes. An unusual feature of the echinomycin–d(CGTACG) complex is the Hoogsteen base pairing of the two central A·T base pairs in which adenosine assumes the syn conformation (Wang et al., 1984). Subsequent NMR solution studies of drug–oligonucleotide complexes have found oligonucleotide sequence and pH to be important factors in determining whether Watson–Crick or Hoogsteen A·T pairs flank the echinomycin bisintercalation site (Gao & Patel, 1988, 1989). Temperature was found to affect the stability of Hoogsteen A·T base pairs in the interior of the echinomycin–d(ACGTACGT) complex (Gilbert et al., 1989). Footprinting methodologies using DNase I (Low et al., 1984) and methidiumpropyl-EDTA–Fe(II) (Van Dyke & Dervan, 1984) further confirm the preference of echinomycin for binding to CpG steps in the nucleotide sequence and reveal that the drug has a minimum binding site size of four base pairs, with the strongest binding to ACGT and TCGT sequences.

[1] Abbreviations: CD, circular dichroism; *D* and *E*, triplet-state zero-field splitting parameters; DNA, deoxyribonucleic acid; EDTA, ethylenediaminetetraacetic acid; HPLC, high-performance liquid chromatography; LPSE, buffer consisting of 2 mM phosphate, 10 mM NaCl, and 0.01 mM EDTA at pH 7; NMR, nuclear magnetic resonance; MIDP, microwave-induced delayed phosphorescence; NOE, nuclear Overhauser effect; ODMR, optical detection of triplet state magnetic resonance; OPC, oligonucleotide purification cartridges; poly(dA·dT), double helix formed by the two homopolymers poly(dA) and poly(dT); poly[d(A-T)$_2$], double helix formed by two chains of alternating A's and T's; poly(dG·dC), double helix formed by the two homopolymers poly(dG) and poly(dC); poly[d(G-C)$_2$], double helix formed by two chains of alternating G's and C's; RNA, ribonucleic acid; SSB protein, single-stranded DNA-binding protein; Trp, tryptophan; zfs, zero-field splitting.

Intercalative binding of echinomycin via the quinoxaline moieties has been a central feature confirmed by several structural studies of echinomycin–DNA complexes. The quinoxaline rings of echinomycin were found to selectively stack between adenine and cytosine bases in the drug–d(ACGT) complex and between thymine and cytosine bases in the drug–d(TCGA) complex (Gao & Patel, 1988). It was postulated that the observation of Hoogsteen A·T base pairs in the d(ACGT) complex may reflect the importance of stacking interactions between the quinoxaline ring and A·T base pairs. The Hoogsteen conformation allows aromatic stacking between the quinoxaline ring of the drug and the pyrimidine ring of the adenine base flanking the intercalation site in the echinomycin–d(CGTACG) complex (Ughetto et al., 1985). However, the interplanar spacing between the unsaturated ring systems was determined to be 3.46 Å in the drug complex, which is slightly greater than the nominal 3.4-Å spacing generally observed in stabilizing intermolecular stacking interactions.

Optical detection of triplet-state magnetic resonance (ODMR) spectroscopy is a sensitive method for obtaining the zfs parameters (*D*- and *E*-values) of an excited triplet state as well as the dynamic properties of the individual spin sublevels. Since these properties are influenced by interactions in which the excited-state probe participates, ODMR finds application as a structural tool. The technique has been successfully employed to elucidate aromatic stacking interactions in the hydrophobic contacts made between SSB proteins and polynucleotide targets (Casas-Finet et al., 1987, 1988). The effect of various specific mutations on the nature of the protein–nucleic acid interactions has allowed assessment of the role of individual Trp residues and their involvement in stacking interactions of SSB proteins (Tsao et al., 1989; Khamis et al., 1987a,b; Zang et al., 1987). Triplet-state spectroscopic evidence from these investigations that points to the presence of Trp–base stacking interactions can be summarized as follows: (1) significantly reduced triplet-state lifetimes of Trp upon stacking with thymine, (2) reduction in the zfs *D* parameter value, (3) red shifts in the phosphorescence origin of Trp upon complexation with poly(dT), and (4) reversal in the polarity of stacked Trp ODMR signals in complexes with poly(dT). Analogous changes in the quinoxaline probe triplet-state properties would prove useful for elucidation of aromatic stacking interactions in echinomycin–nucleic acid complexes.

In this report, triplet-state spectroscopic investigations of echinomycin and echinomycin–DNA complexes were carried out in order to characterize the role of stacking interactions of the drug's quinoxaline moieties upon binding to DNA targets. Low-temperature phosphorescence and ODMR spectroscopy were utilized to investigate environmental perturbations of the quinoxaline chromophores of the drug upon complexation with natural and synthetic DNA polymers. In addition, echinomycin complexes with the short duplex oligonucleotides d(ACGT), d(CGTACG), and d(ACGTACGT), which potentially model drug binding sites, were investigated. Changes in phosphorescence emission characteristics and lifetime, triplet-state zfs parameters, and ODMR spectra were measured upon drug binding to DNA targets.

Experimental Procedures

Sample Preparation. Quinoxaline was purchased from Aldrich Chemical Co., Milwaukee, WI, and purified by recrystallization from petroleum ether and repeated vacuum sublimation. Echinomycin was a gift from the National Cancer Institute and was estimated to be greater than 97%

pure by reversed-phase/UV photodiode array HPLC methods (Alfredson et al., 1990). Double-stranded poly[d(A-T)$_2$], poly(dA·dT), poly[d(G-C)$_2$], and poly(dG·dC) were obtained from Pharmacia Inc., Piscataway, NJ. Calf thymus (highly polymerized sodium salt, type 1), *Micrococcus lysodeikticus*, and *Escherichia coli* DNAs were purchased from Sigma Chemical Co., St. Louis, MO. The polynucleotides were used without further purification. The duplex oligonucleotides d(ACGT), d(CGTACG), and d(ACGTACGT) were produced on a Model 380 DNA synthesizer (Applied Biosystems Inc., Foster City, CA) and subsequently deprotected and purified by means of OPC purification cartridges (Applied Biosystems Inc.) following standard procedures. Oligonucleotide purity was at least 95% as determined by HPLC analysis (Becker et al., 1985).

All spectroscopic measurements were made in a low ionic strength aqueous buffer containing 2 mM phosphate, 10 mM NaCl, and 0.01 mM EDTA at pH 7.0 (LPSE buffer). Sample concentrations were determined spectrophotometrically [echinomycin, ϵ_{325} = 11 500; quinoxaline, ϵ_{314} = 5700; and DNAs, ϵ_{260}(nucleotides) = 6600] by using a Model 8450 UV spectrophotometer (Hewlett-Packard, Palo Alto, CA). Solid echinomycin was shaken in a laboratory mixer with LPSE buffer containing 16% (v/v) ethylene glycol (spectroscopic grade, Mallinckrodt Chemical Co., Milwaukee, WI), which served as a cryosolvent (Brenner et al., 1988). Excess echinomycin was removed by high-speed centrifugation. In this manner, echinomycin concentrations of up to 30 μM could be achieved for spectroscopic measurements of the free drug. Quinoxaline samples were prepared directly in LPSE buffer containing 16% ethylene glycol.

Echinomycin binding to natural and synthetic DNAs was carried out by means of a modified solid-shake procedure (Lee & Waring, 1978). LPSE buffer solution approximately 1 mM in nucleotide was added to a small amount (ca. 0.2 mg) of solid echinomycin. The mixture was then shaken for 2 h in a laboratory shaker at ambient temperature. Excess echinomycin, which has low aqueous solubility, was subsequently removed by high-speed centrifugation. Control samples of solid echinomycin in LPSE buffer without the nucleic acid were shaken, centrifuged, and employed for spectroscopic determination of the concentration of free drug in solution. The concentration of bound drug was measured spectrophotometrically in the drug–DNA solutions by using the weak band of echinomycin at 325 nm, which minimized interference from nucleotide absorbance. In most cases, 90–95% of the echinomycin in solution was the bound form of the drug. The drug's absorbance maxima at 245 and 325 nm were very slightly red-shifted (1–2 nm) upon binding to DNA. Ethylene glycol (16% v/v) was added as a cryosolvent just prior to low-temperature phosphorescence and ODMR spectroscopic measurements. Even though echinomycin complexes exhibit relatively slow dissociation kinetics for most DNAs (Fox et al., 1981), the time between addition of the cryosolvent and sample cooling was kept as short as possible. The effect of the cryosolvent on complex dissociation was negligible under these conditions.

Phosphorescence and ODMR Spectroscopic Methods. Samples were transferred to a 2-mm i.d. Suprasil quartz tube (Heraeus-Amersil, Inc., Sayreville, NJ), inserted into a microwave slow-wave copper helix terminating a coaxial microwave transmission line, and immersed into a dewar for low-temperature phosphorescence and ODMR measurements. Phosphorescence spectra were acquired at 77 and 4.2 K. A rotating can sector with a dead time of about 1 ms was employed to eliminate the fluorescence background. Samples were optically pumped with a 100-W high-pressure Hg arc lamp fitted in a Model ALH-215 housing (Photochemical Research Associates, London, Ontario, Canada). Light from the source was passed through a $NiSO_4$ or $CoSO_4$ solution filter and a Model H-10 10-cm monochromator (Instruments SA, Metuchen, NJ) and then focused onto the sample. An excitation wavelength of 313 nm was commonly employed except for the drug–d(ACGT) and drug–d(ACGTACGT) complexes, which were excited at 365 nm. Emission was viewed at right angles through a WG-345-2 glass filter and a Model 2051 1-m monochromator (GCA/Mc Pherson Instrument Corp., Acton, MA) with detection by a Model 9789QA cooled photomultiplier tube (EMI, Acton, MA). Emission slits were generally set at 3-nm band-pass. Data collection and reduction were carried out by use of a Model TN-1550 signal averager (Tracor Northern, Inc., Middleton, WI) interfaced to a Pro-350 microcomputer (Digital Equipment Corp., Maynard, MA).

Phosphorescence lifetimes were determined from signal-averaged phosphorescence decay measurements at 77 K, where spin–lattice relaxation equalizes the triplet sublevel populations. Decays were deconvoluted by using previously described procedures (Maki & Co, 1976). A nonlinear least-squares Marquardt algorithm designed to minimize χ^2 of the fitting function was employed to calculate preexponential factors and decay constants in a multiexponential analysis. Plots of residuals were used to monitor goodness of fit, which was considered satisfactory when the deviation was ±5% or less.

ODMR slow-passage experiments were performed at pumped liquid helium temperatures (ca. 1.2 K) in order to quench spin–lattice relaxation. Microwave frequencies were generated by a Model 8350B broad-band sweep oscillator (Hewlett-Packard, Palo Alto, CA) fitted with a Model 8359A plug-in amplifier. ODMR spectra were acquired by monitoring the phosphorescence intensity either at the 0,0 band apex or at 488 nm, near the blue edge, while sweeping the microwaves slowly through a pair of triplet sublevels in zero magnetic field. These two conditions select for the red and blue triplet state of echinomycin, respectively. The microwave frequencies that match the energy differences between sublevels induce optically detected magnetic resonance transitions and characterize the zero-field splittings of the triplet state. All ODMR spectra were corrected for rapid passage effects by measurement at several sweep rates and extrapolation of the peak frequency to zero sweep rate.

Wavelength-selected ODMR experiments were performed by observing ODMR signals through the emission monochromator with a narrow optical window (1.5-nm band-pass or less). Spectra were acquired over a range of wavelengths covering the 0,0 band of the emission profile of echinomycin and quinoxaline.

Microwave-induced delayed phosphorescence (MIDP) measurements were performed to obtain the individual sublevel decay rates of the lowest triplet state of echinomycin by using established techniques that have been previously described in detail (Schmidt et al., 1971). Basically, the MIDP methodology employed is a phosphorescence decay measurement at 1.2 K wherein at some delay time, t, a microwave pulse is applied to excite a transition between a sublevel pair (T_x–T_z, T_y–T_z), producing an increase in the phosphorescence intensity (h). If the delay time is sufficiently long to allow the shorter-lived of the two sublevels to empty, h will be proportional to the remaining population in the slowly decaying sublevel. The slope of a plot of the normalized values of log h versus

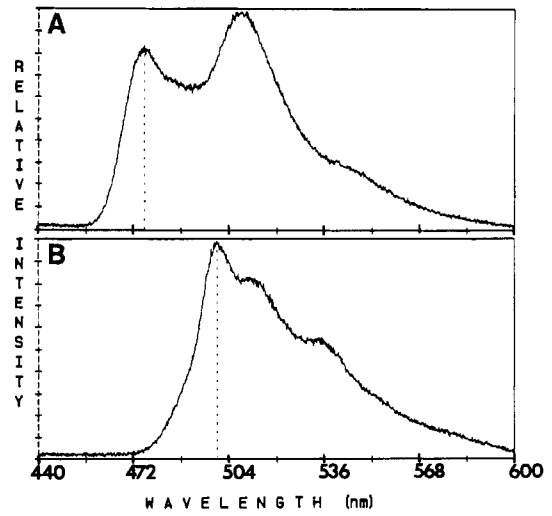

FIGURE 2: Phosphorescence emission spectra at 4.2 K of (A) quinoxaline, 80 μM, and (B) echinomycin, 30 μM, in LPSE buffer containing 16% ethylene glycol. Excitation is at 313 nm.

t will yield the total decay rate constant of that sublevel. In this manner, the decay rate constants for the nonradiative sublevels (k_x, k_y) were determined. The decay rate constants of the radiative sublevel (k_z) were obtained from analysis of the decay profile of the delayed phosphorescence signal at long delay times (>2.5 s).

RESULTS

Triplet-State Properties of Echinomycin. The phosphorescence spectrum of echinomycin in LPSE buffer is shown in Figure 2. A relatively unstructured emission profile is obtained with an apparent 0,0 band maximum at 500.5 nm. Excitation wavelengths from 289 to 365 nm yielded nearly identical spectra. The phosphorescence spectrum of quinoxaline is shown for comparison. A 0,0 band maximum at 476 nm is observed for the parent chromophore.

ODMR investigations of tryptophan phosphorescence emission bands in proteins (von Schütz et al., 1974) have demonstrated that a combination of optical wavelength selection and ODMR can be employed to detect heterogeneity in the emission of tryptophan at different protein sites. By observing ODMR signals through a monochromator at a narrow band-pass, multiple sites are evidenced by discontinuities in a plot of ODMR frequency versus monitored wavelength, provided only a single vibronic band is monitored. This methodology has been successfully employed in recent studies of tryptophan residue heterogeneity in complexes of *E. coli* SSB proteins with single-stranded polynucleotides (Khamis et al., 1987a; Tsao et al., 1989). Wavelength-selected ODMR experiments were conducted on echinomycin in an attempt to elucidate heterogeneity in the phosphorescence emission profile. ODMR spectra were acquired at several wavelengths across the 0,0 band of the drug. Similar experiments were performed on quinoxaline. The zfs and orientation of the principal magnetic axes of quinoxaline in its triplet state are shown in Figure 3. In echinomycin, as in quinoxaline, only the T_z sublevel is detectably radiative and therefore, only two ODMR transitions are observed in the spectrum (a $2E$ signal and a $D + E$ signal). Both signals are of negative polarity (a decrease in phosphorescence intensity upon microwave irradiation) reflecting a higher steady-state population in T_z than in the other sublevels. Figure 4 displays the results of wavelength-selected ODMR measurements for the $2E$ and $D + E$ signals of echinomycin and quinoxaline. Quinoxaline shows the appearance of a second set of ODMR signals at wavelengths to the red of the 0,0 band peak at 476 nm. Each signal depends linearly on the wavelength and displays a nearly identical slope. The observation that the same ODMR frequencies are found in both the red-shifted and blue-shifted signals leads to the following interpretation. At the monitored wavelengths to the blue of the inhomogeneously broadened 0,0 band apex, we observe different populations of emitting triplet states as the wavelength is varied. It is well-known (Gradl et al., 1986; Gradl & Friedrich, 1985; Williamson & Kwiram, 1988) that the solvent-induced Stark shift of the T_1–S_0 energy splitting and of the zfs are correlated, thus giving the linear wavelength dependence. As the monitored wavelength enters a new red-shifted vibronic band, we begin to monitor the *same* populations of emitting triplet states, whose Stark-shifted zfs and T_1–S_0 splitting repeat those monitored previously in the 0,0 band (Kwiram et al., 1978). Thus, the two slopes as well as the range of the zfs should be the same. Furthermore, the energy spacing between the two regression lines should correspond to a known vibronic band splitting. The measured splitting from the $D + E$ transitions of Figure 4 is 530 cm^{-1}, which cannot be resolved as separate bands in the phosphorescence spectrum of Figure 2. A prominent vibronic band at 0,0–528 cm^{-1} has been assigned, however, to a totally symmetric β skeletal distortion mode in the 4.2 K Shpol'skii phosphorescence spectrum of quinoxaline in *n*-

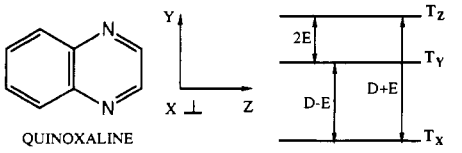

FIGURE 3: Structure of quinoxaline and principal magnetic axis system. Phosphorescence originates exclusively from the T_z sublevel.

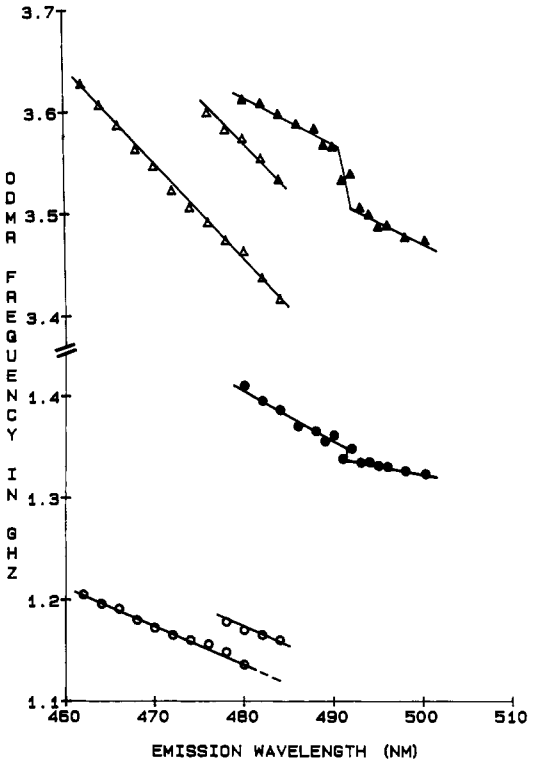

FIGURE 4: ODMR frequency versus emission wavelength for echinomycin and quinoxaline. Sample conditions are given in Figure 2. T = 1.2 K; emission slits are set at 1.5-nm band-pass. Microwave sweep rate is 375 MHz/s (uncorrected for rapid passage effects); (○) quinoxaline $2E$ signal; (●) echinomycin $2E$ signal; (△) quinoxaline $D + E$ signal; (▲) echinomycin $D + E$ signal.

Table I: Triplet-State Properties of Echinomycin and Quinoxaline in Aqueous Solution[a]

sample	phosphorescence decay[b] (s)	ODMR signals[c] (GHz)		zfs parameters[d] (GHz)	
		$2E$	$D + E$	D	E
echinomycin					
λ_{em} = 488 nm (blue)	0.08 (16%) 0.29 (75%) 1.14 (9%)	1.310	3.529	2.874 (±0.013)	0.655 (±0.008)
$\lambda_{0,0}$ = 500.5 nm (red)	0.06 (13%) 0.26 (80%) 1.09 (7%)	1.250	3.357	2.732 (±0.011)	0.625 (±0.006)
quinoxaline					
$\lambda_{0,0}$ = 476 nm	0.28 (99%) 1.33 (1%)	1.121	3.480	2.920	0.560

[a] Sample concentrations were 30 μM echinomycin and 80 μM quinoxaline in LPSE buffer containing 16% ethylene glycol. Excitation was at 313 nm, with emission wavelengths measured at 4.2 K. [b] Decay measurements were made at 77 K and fit to a multicomponent exponential with the preexponential contributions listed in parentheses for each lifetime component. Standard deviation for the lifetime measurements was 0.01 s (n = 5). The ca. 1-s lifetime component is assigned to an impurity present in the solvent. [c] Zero-field ODMR frequencies were measured at 1.2 K and corrected for rapid passage effects. Signals are all of negative polarity. [d] Standard deviations for echinomycin calculated from n = 5 independent measurements are listed in parentheses. The standard deviation of the mean is less by $1/n^{1/2}$.

hexane (Suga & Kinoshita, 1982). Thus the red-shifted set of ODMR signals of quinoxaline can be accounted for readily. Since there is no discontinuity of the zfs versus wavelength *within* the monitored emission of a single vibronic band, we conclude (von Schütz et al., 1974) that the emission originates from a continuous distribution of solvent microenvironments.

The zfs versus wavelength behavior of echinomycin, on the other hand, is clearly different from that of quinoxaline. There is a discontinuity at ca. 490 nm, but the zfs of the signals to the red of the discontinuity do not repeat those observed to the blue. Thus, we are not traversing the same populations via a new vibronic band; rather, a distinct set of populations are being observed. The presence of a discontinuity *within* a vibronic band implies the presence of two resolvable distributions of microenvironments (von Schütz et al., 1974). We interpret these results to mean that the quinoxaline chromophores of echinomycin occupy two (or more) distinguishable conformations that have differing S_0–T_1 energy splittings (see below). This interpretation of the wavelength-dependent ODMR is the basis for our reference to *blue* and *red* triplet states of echinomycin in this report. Correspondingly, all measurements of the triplet-state properties of echinomycin were carried out at both 488 nm (blue triplet state) and at the apparent 0,0 band apex wavelength (red triplet state) in order to discriminate between changes in each triplet-state environment upon binding the drug to nucleic acid targets.

The properties of the blue and red triplet states of echinomycin are listed in Table I along with those of quinoxaline for comparison. The red triplet state of the drug has a slightly shorter major decay component lifetime and lower D and E zfs parameters than the blue triplet state of the drug. The phosphorescence emission spectrum of the drug is red-shifted relative to quinoxaline, and both the red and blue triplet states exhibit a lower D and higher E zfs parameter. These effects probably are due mainly to the presence of the side chain attached at position 2 of the quinoxaline ring in the drug. Possible origins of the two quinoxaline environments of echinomycin will be discussed below.

Echinomycin–Oligonucleotide Complexes. Figure 5 displays the phosphorescence emission spectra of the comlexes of echinomycin with d(ACGT), d(CGTACG), and d(ACGTACGT). An excitation wavelength of 313 nm was employed for the hexamer complex. The d(ACGT) and d(ACGTACGT) complexes, however, exhibited a strong phosphorescence band to the blue of the phosphorescence of echinomycin, which was reduced by excitation at 365 nm. The emission to the blue of the phosphorescence of echinomycin

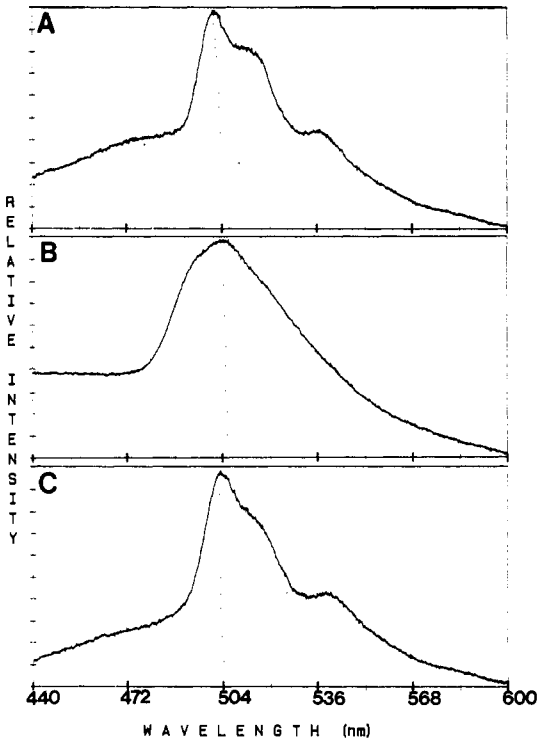

FIGURE 5: Phosphorescence spectra of echinomycin–oligonucleotide complexes; T = 4.2 K. (A) Echinomycin–d(ACGT) complex; (B) echinomycin–d(CGTACG) complex; (C) echinomycin–d(ACGTACGT) complex. Excitation is at 365 nm for (A) and (C) and at 313 nm for (B).

(432-nm band maximum at 313-nm excitation) was found to originate largely from the oligonucleotides. Cursory ODMR measurements (data not shown) indicate that the blue emission band stems from thymine and possibly adenine in the d(ACGT) and d(ACGTACGT) complexes. Since the d(CGTACG) complex displays a much weaker blue phosphorescence band, it appears that thymine (and possibly adenine) bases at the ends of the DNA tetramer and octamer may be largely responsible for the blue emission band observed upon excitation at 313 nm. A slight red shift (1–4 nm) of the 0,0 band peak of echinomycin is observed upon complexation with these oligonucleotides. The drug–d(CGTACG) complex yields a broader, less structured phosphorescence than either the drug itself or the other DNA complexes.

ODMR spectra of echinomycin and its oligonucleotide complexes were acquired for both the blue and red triplet states

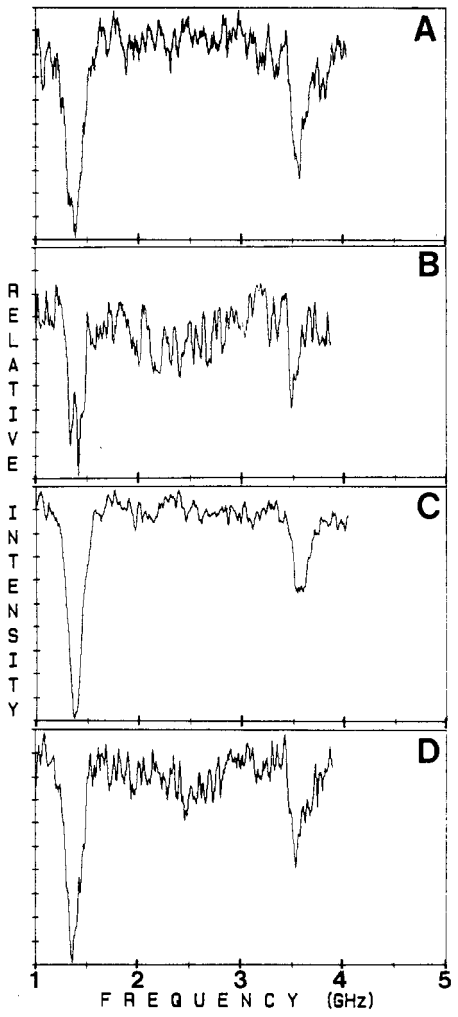

FIGURE 6: ODMR spectra of echinomycin–oligonucleotide complexes: echinomycin blue triplet state. Excitation is at 313 nm; emission is monitored at 488 nm. Microwave sweep rate is 375 MHz/s; T = 1.2 K. (A) Echinomycin; (B) echinomycin–d(ACGT) complex; (C) echinomycin–d(CGTACG) complex; (D) echinomycin–d(ACGTACGT) complex.

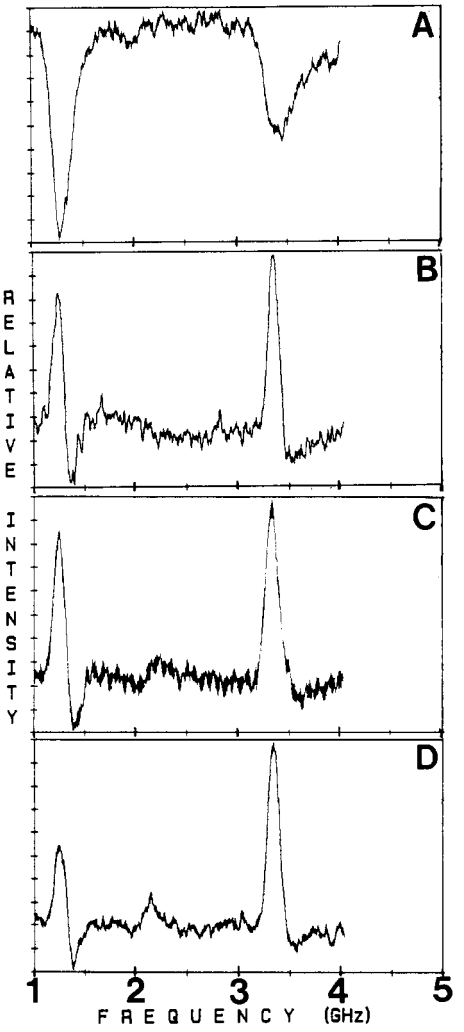

FIGURE 7: ODMR spectra of echinomycin–oligonucleotide complexes: echinomycin red triplet state. Excitation is at 313 nm unless otherwise indicated; emission is monitored at the 0,0 band apex. Microwave sweep rate is 375 MHz/s; T = 1.2 K. (A) Echinomycin; (B) echinomycin–d(ACGT) complex; (C) echinomycin–d(CGTACG) complex; (D) echinomycin–d(ACGTACGT) complex. Excitation is at 365 nm for (B) and (D).

of the drug (Figures 6 and 7, respectively). The blue triplet state of echinomycin (Figure 6) exhibits a slight increase in the frequency of the $2E$ transition as well as a slight decrease in the $D + E$ transition frequency (with the exception of the DNA hexamer complex, in which this transition frequency increases) upon oligonucleotide complexation. The blue triplet-state ODMR transitions in the drug–d(CGTACG) complex are much more intense than those of the other DNA complexes. The ODMR spectra of the red triplet state of echinomycin (Figure 7) displays several distinctive changes upon binding to the oligonucleotides. Most notably, both the $2E$ and $D + E$ transitions undergo a reversal in signal polarity upon complexation. Additionally, a weak $D - E$ signal is observed for both the DNA hexamer and octamer complexes. Both the $2E$ and $D + E$ transitions of the red triplet state shift to lower frequency upon complexation. The negative component seen at a higher frequency, most noticeable in the $2E$ transitions and to a lesser extent in the $D + E$ transitions, arises from the blue triplet state, whose phosphorescence overlaps that of the red site. The contribution of free echinomycin remaining in solution to the ODMR spectra of the drug–DNA complexes is small due to its low concentration and, in many cases, weaker, broader signals.

The properties of the blue and red triplet states of echinomycin and its oligonucleotide complexes are summarized in Tables II and III, respectively. The blue triplet state of echinomycin (Table II) undergoes a decrease in the zfs D-value upon binding to the DNA tetramer and octamer. By contrast, no change in the D parameter is observed upon formation of the drug–d(CGTACG) intercalation complex. No significant change in the E parameter occurs upon binding to the oligonucleotides. Phosphorescence lifetime measurements of the drug in the tetramer and octamer complexes were precluded by the oligonucleotide emission at 488 nm, but a small increase in the major decay component appears to occur upon binding to the hexamer. The red triplet state of echinomycin (Table III) exhibits a small decrease (8–15%) in the lifetime of the major decay component and a reduction in both D and E upon binding to the oligonucleotide targets. Each of these effects is consistent with stacking interactions that reduce the dipolar coupling of the unpaired electrons, whose wave function expands in a more polarizable environment, and that also may introduce charge-transfer character into the quinoxaline triplet state (McGlynn et al., 1969; Iwata et al., 1967; Hayashi et al., 1969; Mohwald & Sackmann, 1974; Krebs et al., 1971; Schweitzer et al., 1976).

Echinomycin–Polymeric DNA Complexes. The phosphorescence emission spectra of several polymeric DNA complexes of echinomycin are shown in Figure 8. A slight

Table II: Triplet-State Properties of Echinomycin–Oligonucleotide Complexes: Blue Triplet State of Echinomycin[a]

sample	phosphorescence decay[b] (s)	ODMR signals[c] (GHZ)		zfs parameters (GHz)		ΔD[d] (MHz)
		$2E$	$D + E$	D	E	
echinomycin	0.08 (16%) 0.29 (75%) 1.14 (9%)	1.310	3.529	2.874 (±0.013)	0.655 (±0.008)	
echin–d(ACGT)	*e*	1.318	3.485	2.826	0.659	−48
echin–d(CGTACG)	0.10 (17%) 0.31 (70%) 1.09 (13%)	1.321	3.535	2.874	0.661	0
echin–d(ACGTACGT)	*e*	1.328	3.513	2.849	0.664	−25

[a] Samples were dissolved in LPSE buffer containing 16% ethylene glycol. Excitation was at 313 nm, and emission was monitored at 488 nm. [b] Decay was measured at 77 K and fit to a multicomponent exponential with preexponential contributions listed in parentheses for each lifetime component. [c] Zero-field ODMR frequencies were measured at 1.2 K and are corrected for rapid passage effects. All signals have negative polarity. [d] Shift of zfs D-value upon binding to oligonucleotide targets. [e] Not measured due to emission background interference from oligonucleotides.

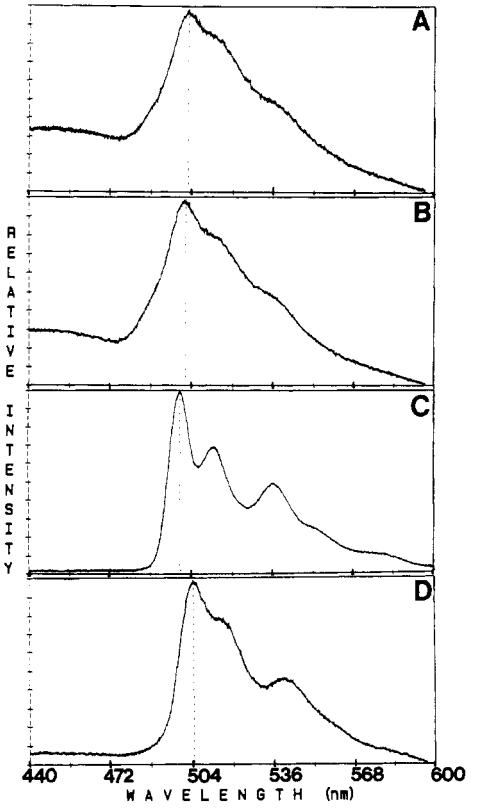

FIGURE 8: Phosphorescence spectra of echinomycin–polymeric DNA complexes. Excitation is at 313 nm; T = 4.2 K. (A) Echinomycin–poly(dG·dC) complex: (B) echinomycin–poly[d(G-C)$_2$] complex; (C) echinomycin–poly[d(A-T)$_2$] complex; (D) echinomycin–*M. lysodeikticus* DNA complex.

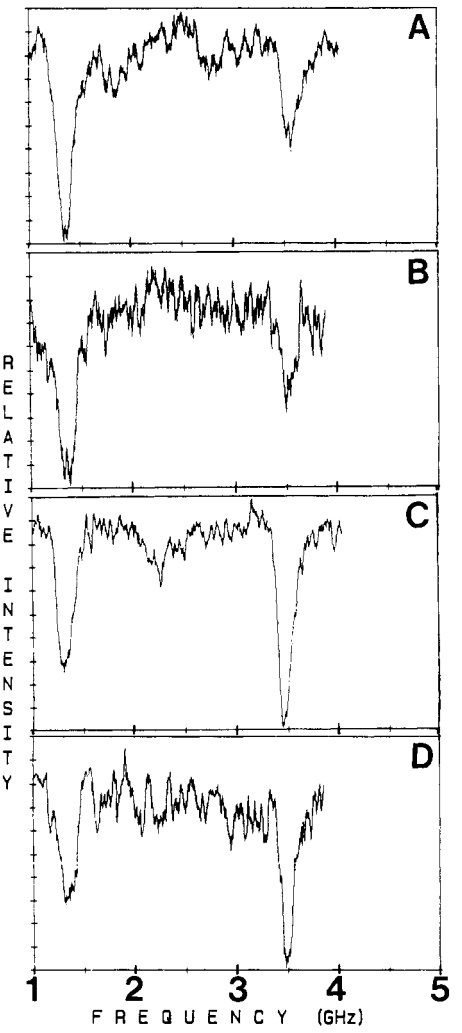

FIGURE 9: ODMR spectra of echinomycin–polymeric DNA complexes: echinomycin blue triplet state. Excitation is at 313 nm; emission is monitored at 488 nm. Microwave sweep rate is 375 MHz/s; T = 1.2 K. (A) Echinomycin–poly(dG·dC) complex; (B) echinomycin–poly[d(G-C)$_2$] complex; (C) echinomycin–poly[d(A-T)$_2$] complex; (D) echinomycin–*M. lysodeikticus* DNA complex.

red shift (1–4 nm) of the phosphorescence maximum of the drug occurs upon binding, with the exception of the echinomycin–poly[d(A-T)$_2$] complex, for which a very small blue shift is observed along with enhanced resolution of the vibronic manifold. A very small blue shift is also observed for the drug–poly(dA·dT) complex. Although only the drug–*M. lysodeikticus* DNA complex is shown in Figure 8, the spectra of the other natural DNA complexes are very similar.

Figure 9 displays the ODMR spectra of the blue triplet state of several polymeric DNA complexes of echinomycin. In general, both the $2E$ and $D + E$ transitions of the drug shift to lower frequencies upon complexation with the DNAs. For the echinomycin–poly[d(A-T)$_2$] complex, a weak $D - E$ signal also is observed in the ODMR spectrum. All signals are of negative polarity. The ODMR spectra of the red triplet state of several polymeric DNA complexes of echinomycin are shown in Figure 10. As with the drug's blue triplet state, the red triplet state exhibits a decrease in the $D + E$ transition frequency upon binding to the polymeric DNAs, with the exception of the poly[d(G-C)$_2$] complex, for which an increase in $D + E$ transition frequency is found. Also, no significant change in frequency is observed for the $D + E$ signal of the drug–poly(dA·dT) complex. Slight decreases are observed for most $2E$ transition frequencies upon binding of the drug, with

Table III: Triplet-State Properties of Echinomycin–Oligonucleotide Complexes: Red Triplet State of Echinomycin[a]

sample	$\lambda_{0,0}$ (nm)	phosphorescence decay[b] (s)	ODMR signals[c] (GHz) 2E	ODMR signals[c] (GHz) D + E	zfs parameters (GHz) D	zfs parameters (GHz) E	ΔD[d] (MHz)
echinomycin	500.5	0.06 (13%) 0.26 (80%) 1.09 (7%)	1.250	3.357	2.732 (±0.011)	0.625 (±0.006)	
echin–d(ACGT)	501.5[e]	0.04 (11%)[e] 0.24 (61%) 1.10 (28%)	1.206 (+)	3.295 (+)	2.692	0.603	−40
echin–d(CGTACG)[f]	504.2	0.03 (7%) 0.22 (73%) 0.78 (20%)	1.202 (+)[e]	3.278 (+)[e]	2.677	0.601	−55
echin–d(ACGTACGT)	503.1[e]	0.04 (7%)[e] 0.22 (79%) 0.91 (14%)	1.202 (+)	3.292 (+)	2.691	0.601	−41

[a] Samples were dissolved in LPSE buffer containing 16% ethylene glycol. Excitation is at 313 nm, unless otherwise indicated. 0,0 band peak wavelengths were recorded at 4.2 K. [b] Decays were measured at 77 K and fit to a multicomponent exponential with preexponential contributions listed in parentheses for each lifetime component. The long-lived component in the complexes is assigned largely to oligonucleotide phosphorescence. [c] Zero-field ODMR frequencies were measured at 1.2 K and corrected for rapid passage effects. (+) indicates that a positive polarity ODMR signal was observed. A $D - E$ signal at 2.095 GHz was observed for the echinomycin–d(ACGTACGT) complex. [d] Change in zfs D-value upon binding to oligonucleotide targets. [e] Excitation was at 365 nm. [f] A weak $D - E$ signal was observed at ca. 2.1 GHz.

the exception of the alternating synthetic copolymer complexes. The most notable changes in the red triplet-state ODMR spectra of echinomycin are the polarity reversals of both the $2E$ and $D + E$ signals upon complexation with all the natural DNAs investigated in this study and with the poly[d(A-T)$_2$] complex. The homopolymer duplexes and poly[d(G-C)$_2$] yielded negative polarity ODMR signals upon drug complexation. The reversal of ODMR signal polarity is similar to that observed in complexes with the model duplex oligonucleotides (Figure 7). Additionally, a pronounced $D - E$ signal appears in the ODMR spectrum of the poly[d(A-T)$_2$] complex. Qualitatively, there is a striking resemblance between the changes in the drug's red triplet state upon binding to poly[d(A-T)$_2$] and upon complexation with the natural DNAs. The negative component observed on the high-frequency edge of the ODMR signals of the poly[d(A-T)$_2$] and the natural DNA complexes originates from the overlapping blue triplet-state transitions.

In an effort to shed light on the reversal of ODMR signal polarity of the red triplet state of echinomycin upon binding with poly[d(A-T)$_2$] and the natural DNAs, individual triplet sublevel decay rate constants were measured for several DNA complexes by using MIDP. A summary of the individual sublevel kinetics of the red triplet state of echinomycin and its polymeric DNA complexes is given in Table IV. In addition, the triplet sublevel kinetics of quinoxaline in ethanol, hexane, and naphthalene-d_8 are also included in the table for comparison. The upper and lower limits for the relative populating rates were calculated from measured sublevel decay rate constants and the experimentally observed polarity of the ODMR signals, assuming that only the T_z sublevel is radiative and that spin–lattice relaxation is negligible. The average sublevel lifetimes calculated from the decay rates listed in Table IV are in agreement with the lifetimes of the major components observed at 77 K (see below). As can be seen in the table, the T_z sublevel decay constants are significantly enhanced and the T_x and T_y decay constants are reduced upon binding of echinomycin to poly[d(A-T)$_2$] and to the natural DNAs. In contrast, the poly(dG·dC) and poly[d(G-C)$_2$] complexes exhibit an increase in the T_x sublevel decay constants and only a minor increase in the T_z decay constants relative to the free drug. The calculated upper and lower limits of the relative populating rates for all the complexes yield a consistent set of values [p_x:p_y:p_z ranges of 0.05–0.08: 0.11–0.19:1.0 would satisfy all the calculated limits with the exception of the lower limit of p_y calculated for the echinomycin–poly(dG·dC) complex]. Similar trends were noted for the blue triplet-state kinetics of echinomycin upon binding to polymeric DNAs (data not shown). However, the variation

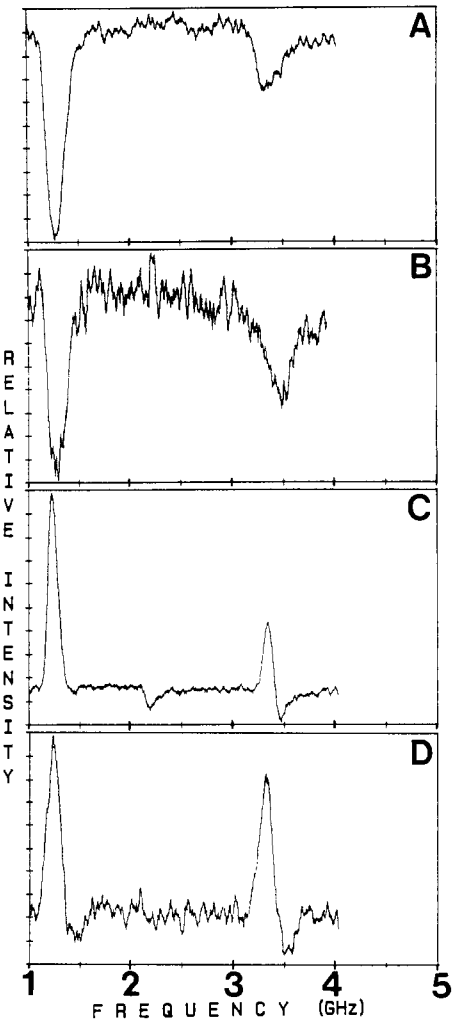

FIGURE 10: ODMR spectra of echinomycin–polymeric DNA complexes: echinomycin red triplet state. Excitation is at 313 nm; emission is monitored at the 0,0 band peak. Microwave sweep rate is 375 MHz/s; T = 1.2 K. (A) Echinomycin–poly(dG·dC) complex; (B) echinomycin–poly[d(G-C)$_2$] complex; (C) echinomycin–poly[d(A-T)$_2$] complex; (D) echinomycin–*M. lysodeikticus* DNA complex.

Table IV: Triplet-State Kinetics of Echinomycin–Polymeric DNA Complexes: Red Triplet State of Echinomycin[a]

sample	sublevel decay rates[b] (s^{-1})			relative populating rates[c]		
	k_x	k_y	k_z	p_x	p_y	p_z
echinomycin	0.70 (±0.05)	1.58 (±0.09)	9.2 (±0.3)	≤0.07	≤0.17	1.0
echin–poly[d(G-C)$_2$]	0.88	1.94	9.8	≤0.08	≤0.19	1.0
echin–poly(dG·dC)	0.93	0.99	10.5	≤0.08	≤0.09	1.0
echin–poly[d(A-T)$_2$]	0.58	1.34	11.9	≥0.05	≥0.12	1.0
echin–*M. lysodeikticus* DNA	0.57	1.27	12.2	≥0.05	≥0.11	1.0
echin–*E. coli* DNA	0.64	1.25	12.3	≥0.06	≥0.11	1.0
quinoxaline						
in ethanol[d]	1.2	1.3	6.5	0.056	≤0.20	1.0
in hexane[e]	0.86	1.14	12.3	0.045	0.084	1.0
in naphthalene-d_8[f]	0.42	0.80	12.0	0.013	0.024	1.0

[a] Samples were dissolved in LPSE buffer containing 16% ethylene glycol. Excitation was at 313 nm, and emission was monitored at wavelengths slightly to the red of the apparent 0,0 band maximum. [b] The k_u (u = x, y, z) values are apparent total decay rate constants obtained from MIDP measurements at 1.2 K. Standard deviations for echinomycin calculated from $n = 3$ independent measurements are listed in parentheses. [c] The p_u (u = x, y, z) values are calculated from the measured decay rates and the experimentally observed polarity of the ODMR signals. [d] Data from Inoue et al. (1980). [e] Data from Suga and Kinoshita (1982). [f] Data from Schmidt et al. (1971).

Table V: Triplet-State Properties of Echinomycin–Polymeric DNA Complexes: Blue Triplet State of Echinomycin[a]

sample	phosphorescence decay[b] (s)	ODMR signals[c] (GHz)		zfs parameters (GHz)		ΔD[d] (MHz)
		$2E$	$D + E$	D	E	
echinomycin	0.08 (16%) 0.29 (75%)	1.310	3.529	2.874 (±0.013)	0.655 (±0.008)	
echin–poly(dG·dC)	0.07 (16%) 0.29 (73%)	1.292	3.506	2.860	0.646	−14
echin–poly(dA·dT)	0.07 (9%) 0.30 (83%)	1.357	3.487	2.809	0.678	−65
echin–poly[d(G-C)$_2$]	0.07 (18%) 0.30 (72%)	1.294	3.490	2.843	0.647	−31
echin–poly[d(A-T)$_2$][e]	0.06 (17%) 0.29 (72%)	1.270	3.407	2.772	0.635	−102
echin–*M. lysodeikticus* DNA	0.07 (18%) 0.29 (72%)	1.333	3.450	2.783	0.667	−91
echin–*E. coli* DNA	0.07 (19%) 0.29 (69%)	1.322	3.476	2.815	0.661	−59
echin–calf thymus DNA	0.07 (23%) 0.29 (58%)	1.306	3.475	2.822	0.653	−52

[a] Samples were dissolved in LPSE buffer containing 16% ethylene glycol. Excitation was at 313 nm, and emission was monitored at 488 nm. [b] Decay was measured at 77 K and fit to a multicomponent exponential with preexponential contributions listed in parentheses for each lifetime component. A weak, ca. 1-s component attributed to a solvent impurity is omitted from the table. [c] Zero-field ODMR frequencies were measured at 1.2 K and corrected for rapid passage effects. All signals have negative polarity. [d] Change in zfs D-value upon binding to DNA targets. [e] A $D - E$ signal was obtained at 2.15 GHz.

in sublevel decay rate constants upon binding were much smaller than those observed for the red triplet state of the drug.

Table V lists the phosphorescence emission characteristics, ODMR transition frequencies, and D and E parameters of the blue triplet state of echinomycin and its polymeric DNA complexes. Also listed are the changes in zfs D-values upon complexing with DNA. No significant change in phosphorescence lifetime of the major decay component is observed for the blue triplet state of the drug upon binding to the polymeric DNAs. The D parameter decreases upon binding to the DNA targets, with the most significant changes occurring with the poly[d(A-T)$_2$] and *M. lysodeikticus* DNA complexes (−102 and −91 MHz, respectively). The E parameter generally experiences small shifts both to lower and higher values upon DNA complexation.

A summary of the properties of the red triplet state of echinomycin–polymeric DNA complexes is given in Table VI. Binding constants determined for the DNA targets by a solvent partitioning method (Wakelin & Waring, 1976) are also included in this table. The phosphorescence emission lifetime of the major decay component of the drug's red triplet state exhibits a small but significant decrease (up to 15%) upon binding to the polymeric DNAs, with the shortest lifetimes occurring in complexes with the natural DNAs. These results are consistent with the individual sublevel kinetics presented in Table IV. No significant change in the phosphorescence lifetime is observed for the red triplet state of the drug–poly(dA·dT) complex. A significant decrease in the D parameter of the red triplet state occurs upon binding to every DNA target except poly(dA·dT), which produces an insignificant change, and poly[d(G-C)$_2$], for which a significant increase (+48 MHz) is measured. The largest phosphorescence red shift, decrease in phosphorescence lifetime, and reduction in D parameter of the red triplet state occurs upon binding to *M. lysodeikticus* DNA, which also exhibits the highest binding affinity of the nucleic acid targets studied in this work. Apart from the value for the poly[d(G-C)$_2$] complex, for which conformational effects may play a role, a relationship appears to exist between the change in D parameter of the red triplet state of echinomycin upon binding and the binding affinity (Figure 11). The D parameter exhibits lower values as the binding strength of the drug increases for the DNA targets. There appears to be no relationship, however, between the blue triplet-state D parameter and DNA binding affinity.

Discussion

Triplet-State Properties of Echinomycin in Aqueous Solution. Due to the lack of a fluorescent chromophore and the poor solubility of the free drug in aqueous solutions, few

Table VI: Triplet-State Properties of Echinomycin–Polymeric DNA Complexes: Red Triplet State of Echinomycin[a]

sample	$\lambda_{0,0}$ (nm)	phosphorescence decay[b] (s)	ODMR signals[c] (GHz)		zfs parameters (GHz)		ΔD[d] (MHz)	K_0[e] (10^{-5} M^{-1})
			$2E$	$D+E$	D	E		
echinomycin	500.5	0.06 (13%) 0.26 (80%)	1.250	3.357	2.732 (±0.011)	0.625 (±0.006)		
echin–poly(dG·dC)	502.0	0.05 (3%) 0.24 (88%)	1.265	3.302	2.669	0.635	−63	15.1
echin–poly(dA·dT)	498.6	0.27 (94%)	1.293	3.375	2.728	0.647	−4	<0.1
echin–poly[d(G-C)$_2$]	501.5	0.03 (3%) 0.24 (90%)	1.234	3.397	2.780	0.617	+48	5.5
echin–poly[d(A-T)$_2$][f]	500.0	0.02 (3%) 0.22 (88%)	1.190 (+)	3.290 (+)	2.695	0.595	−37	3.1
echin–*M. lysodeikticus* DNA	504.0	0.01 (1%) 0.22 (86%)	1.204 (+)	3.265 (+)	2.663	0.602	−69	31.0
echin–*E. coli* DNA	503.0	0.02 (3%) 0.22 (90%)	1.185 (+)	3.278 (+)	2.685	0.593	−47	9.8
echin–calf thymus DNA	502.5	0.04 (6%) 0.23 (85%)	1.180 (+)	3.282 (+)	2.692	0.590	−40	5.5

[a] Samples were dissolved in LPSE buffer containing 16% ethylene glycol. Excitation was at 313 nm. [b] Decay was measured at 77 K and fit to a multicomponent exponential with preexponential contributions listed in parentheses for each lifetime component. A minor ca. 1-s component attributed to an impurity in the solvent is omitted from the table. [c] Zero-field ODMR frequencies were measured at 1.2 K and corrected for rapid passage effects. Signals have negative polarity unless indicated by (+). [d] Change in D-value upon binding to polynucleotide targets. [e] Binding constants taken from Wakelin and Waring (1976). [f] A $D - E$ ODMR signal is observed at 2.120 GHz.

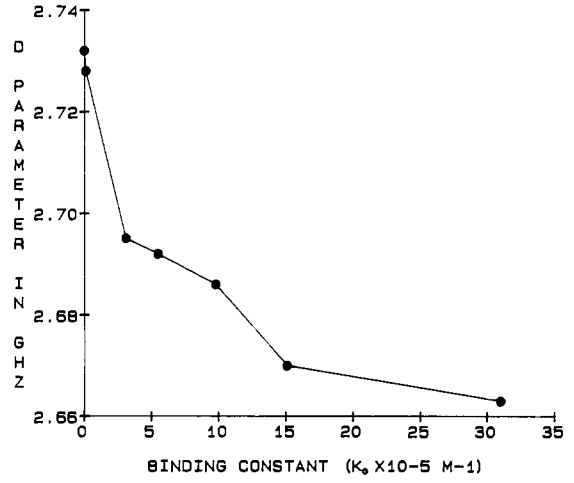

FIGURE 11: D-values of the red triplet state of echinomycin versus binding affinity for polymeric DNA complexes. Binding constants are taken from Wakelin and Waring (1976).

spectroscopic studies have been reported on unbound echinomycin in aqueous environments. The optical absorbance of the quinoxaline chromophore of the drug has been used in low ionic strength aqueous buffer to study the equilibrium binding of echinomycin to DNAs by a solvent partitioning method (Waring & Wakelin, 1976). Recent NMR studies (Gao & Patel, 1988, 1989; Gilbert et al., 1989) as well as CD first-neighbor analysis studies of intercalation site specificities (Jones et al., 1987) have primarily focused on the structure of the complex and changes in nucleic acid targets upon binding in aqueous solutions. Echinomycin conformation in aqueous environments has not been examined directly, but it has been inferred from NMR solution studies in polar solvents such as dimethyl-d_6 sulfoxide (Cheung et al., 1978). The drug has been found to contain substantial symmetry with the exception of the asymmetrical nature of the thioacetal cross-bridge. The two quinoxaline moieties are spaced 10.2 Å apart and are roughly parallel to each other on the same side of the peptide ring on the basis of the calculated minimum-energy conformation. The drug has not been successfully crystallized as yet, although its complex with the DNA hexamer d-(CGTACG) has been studied by single-crystal diffraction techniques (Ughetto et al., 1985).

Wavelength-selected ODMR investigations of echinomycin in LPSE buffer with 16% ethylene glycol described above indicate that the drug contains two distinct triplet states (blue and red triplet states), as evidenced by discontinuities in the plots of ODMR transition frequencies versus monitored emission wavelength. The blue triplet state of echinomycin has a D parameter that is 142 MHz higher and an E parameter that is 30 MHz higher than the corresponding D and E parameters for the red triplet state. The fact that each triplet state of the drug is influenced independently in its interactions with nucleic acid targets further supports the existence of two distinct triplet states of the drug under the conditions of this study. The blue and red triplet states of echinomycin may originate from one of the following possibilities: (1) Since there are two nearly, but not quite, equivalent quinoxalines per drug molecule, the triplet-state properties of each may differ in the unbound form of the drug. (2) The drug may possess a localized triplet state and a triplet state arising from a delocalization over both chromophores. (3) More than one distinct drug conformation may exist in aqueous solutions such that the quinoxaline chromophores of each conformation reside in distinct environments. Due to the high degree of symmetry of the drug, it seems unlikely that the quinoxaline moieties of the drug molecule would exhibit such a large difference in zfs parameters. The second possibility for the origin of the red and blue triplet states of echinomycin (localized and delocalized triplet states) is a more reasonable postulate. ODMR investigations of the double molecule 2,2′-biquinoline in a mixed crystal (Clarke et al., 1982) have shown evidence for the existence of two close-lying triplet states (unresolved in phosphorescence). Each ODMR transition was doubled. On the basis of hyperfine structure analysis, one triplet state was characterized as a localized triplet state with ODMR transitions very close to those of isolated quinoline, while the other triplet state possessed a delocalized character and had ODMR transition frequencies 40–200 MHz lower than those of quinoline. Investigations on an analogous 2,2′-biquinoxaline system revealed similar behavior. In echinomycin, however, due to the considerable separation of the chromophores, it seems unlikely that delocalization over the drug molecule would occur. We think that a likely origin of the two triplet states of echinomycin in aqueous environments is the occurrence of two distinct conformations of the drug that bind

differently to nucleic acid targets. A possibility worth considering is that more than one orientation of the quinoxaline ring may exist in solution due to rotation around the carbon–carbon bond linking the ring and the neighboring amide carbonyl as follows:

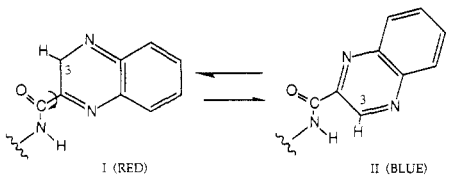

I (RED) II (BLUE)

The two possible local isomeric forms of each quinoxaline could lead to the freezing out of four possible echinomycin conformers at low temperature and/or when a bisintercalation complex is formed with DNA. On the basis of the chemical shifts observed when $Eu(fod)_3$ binds to quinoxaline-2-carboxamide and its extremely close replication of both the proton and C^{13} NMR spectra of echinomycin's quinoxaline moieties, structure I has been suggested to be the major conformation of the drug in polar solvents (Cheung et al., 1978). If the red triplet state of echinomycin is assumed to arise from structure I, then its smaller zfs *D*-value compared with that of the blue triplet state (structure II) may be accounted for by increased conjugation with the side chain. Steric repulsion would be expected in structure II, preventing the amide and aromatic ring from becoming coplanar. In addition, hydrogen bonding between the amide and quinoxaline ring N-atom in structure I could cause a reduction in the zfs *D*-value. Hydrogen bonding of quinoxaline and several related 1,4-diazaaromatics leads to a decrease in the *D* parameter (Chodkowska et al., 1977). Weak hydrogen-bond formation between the quinoxaline ring N-atoms and nearby alanine NH groups has been observed in the crystal structure of the related quinoxaline antibiotic triostin A (Sheldrick et al., 1984). The large differences in quinoxaline ring orientation between the two structures could be responsible for the independent interactions with nucleic acid targets observed for the red and blue triplet states of echinomycin. Recent NMR studies on actinomycin D–d(ATCGAT) intercalation complexes (Zhou et al., 1989) have implicated different chromophore orientations relative to the DNA bases to be a factor in the multiple complexes noted between the drug and oligonucleotide target at temperatures below 20 °C. At higher temperatures, exchange between forms became fast enough that only an average signal was observed.

Echinomycin–DNA Complexes. Echinomycin bisintercalation complexes with the duplex oligonucleotides studied in this report appear to be reasonable models for drug binding to the natural DNAs on the basis of the similarity of changes observed in triplet-state properties of the drug upon complexation. Several quantitative differences are apparent, however, between the ODMR spectra of the model oligonucleotide complexes and those of the natural DNA complexes. The echinomycin–d(CGTACG) complex is unusual in that the negative ODMR signals are more intense, show no change in *D* parameter compared with the free drug, and display greater spectral overlap with the positive ODMR signals compared with the other complexes. Additionally, the phosphorescence emission spectrum for this complex is broader than those of the other nucleotide complexes. The negative ODMR signals for the drug–d(CGTACG) complex do not originate from the unbound drug, since greater than 90% of the drug in solution was calculated to be bound to the DNA. For this complex, the blue triplet-state properties of the drug may be associated with the more solvent-exposed quinoxaline rings on the outside of the stack (rather than a minor form of the drug), consistent with the crystal structure for the intercalation complex (Ughetto et al., 1985). Since any change in *D*-value of this triplet state that occurs upon binding is very small, it appears that intercalation rather than mere stacking with base pairs is required for a reduction in the *D*-value. On the other hand, the ODMR spectrum of the red triplet state is extremely similar to that of the drug in complexes with the natural DNAs. We postulate that in the DNA hexamer–echinomycin complex these signals arise from the quinoxaline moieties that are intercalated.

The echinomycin triplet-state properties in bisintercalation complexes with the d(ACGT) and d(ACGTACGT) oligonucleotides are very similar to those of the drug in complexes with the natural DNAs. Both the blue and red triplet states of the drug undergo similar changes in complexes with these oligonucleotides as they do with the natural DNAs. Qualitatively, a small change in the relative intensities of the $2E$ and $D + E$ signals in the ODMR spectra of the red triplet state of both oligonucleotide complexes along with the appearance of a weak $D - E$ signal in the red triplet-state spectrum of the DNA octamer complex are the only differences that are evident.

Among the echinomycin–polymeric DNA complexes investigated in this report, the differences between the synthetic DNAs and the natural DNAs are very revealing. Although binding affinities indicate a preference of the drug for DNAs of high G+C content, the changes in triplet-state properties upon binding to the natural DNAs resemble those of the poly[d(A-T)$_2$] complex to a greater extent than any of the other synthetic DNA polymers investigated. Echinomycin displays only weak binding to poly(dA·dT), a trait it shares with several other intercalating drugs (Bresloff & Crothers, 1981; Chaires, 1983; Wilson et al., 1985; Strum, 1982). The red triplet state of echinomycin shows no evidence of stacking interactions with poly(dA·dT), which may reflect the weak binding of the drug's major form. A predominant feature of the red triplet state of echinomycin upon binding to the natural DNAs and to poly[d(A-T)$_2$] is the reversal of ODMR signal polarity, which is accompanied by a significant reduction in the zfs *D*-value. The ODMR signal polarity reversal, which was not found for the other synthetic polynucleotides investigated, reflects the triplet sublevel population shifts that accompany drug binding. The reversal of ODMR signal polarity of the red triplet state of echinomycin was also observed upon drug binding to the model oligonucleotides investigated in this study. The results obtained for these echinomycin–DNA complexes suggest that a special interaction of the quinoxaline chromophores with A·T base pairs takes place upon drug binding to the natural DNAs. This interaction between A·T base pairs and the quinoxaline rings of echinomycin may account in part for the TCGT and ACGT preferred recognition sites revealed by footprinting investigations (Van Dyke & Dervan, 1984). Stacking interactions between the drug's quinoxaline rings and A·T pairs flanking the intercalation sites may enhance the stability of drug–DNA complexes.

Measurements of the sublevel decay rate constants for the red triplet state of echinomycin reveal a consistent trend in the changes observed upon drug binding to poly[d(A-T)$_2$] and to the natural DNAs that is not observed with the other drug–polymeric DNA complexes. The nonradiative sublevel decay constants (k_x, k_y) are reduced while the radiative sublevel decay constants (k_z) are significantly enhanced upon complexation (see Table IV). This same trend in sublevel decay constants is found upon changing quinoxaline from a

polar (ethanol) to a nonpolar (hexane or naphthalene) environment. A significant increase of the T_z decay constant results from enhanced spin–orbit coupling between $^3\pi\pi^*$ and $^1n\pi^*$ states of the heterocycle in nonpolar solvents (van der Waals & de Groot, 1967). The energy gap between these states is decreased, and thus their mixing is increased, when the polarity of the environment is reduced. The upper and lower limits of the relative populating rates calculated for the red triplet state of echinomycin suggests that the relative populating rates may not change very much upon binding to the polymeric DNAs. For example, p_x:p_y:p_z values of 0.065:0.15:1.0 (midpoints of the calculated ranges) would satisfy all the calculated upper and lower limits except that of p_y for the drug–poly(dG·dC) complex, which appears to be anomalously small. These results imply that the triplet sublevel population changes of the red triplet state of echinomycin that account for the ODMR signal reversal observed upon drug binding to poly[d(A-T)$_2$] and the natural DNAs are caused primarily by changes in the sublevel decay rate constants of the drug.

We have attempted to model the reversal of ODMR signal polarity observed in the red triplet state of the drug spectra upon complexation with the natural DNAs by varying the solvent environment of quinoxaline itself (data not shown). Although negative polarity signals are observed for the ODMR spectra of quinoxaline in several hydrocarbon solvents as well as in the aqueous solvent system employed in this work, positive polarity signals are induced upon addition of water as an impurity (ca. 0.1% v/v) to an *n*-octane solution of quinoxaline. Since only negative signals are obtained for the ODMR spectrum of quinoxaline in LPSE buffer over a pH range of 2.5–10.5, it appears that the reversal of signal polarity is not simply the result of protonation in the excited state. Possibly, the positive polarity of ODMR signals for quinoxaline are the result of a hydrophobic environment with a highly local polar interaction. A similar environment might occur for the quinoxaline chromophores of echinomycin upon bisintercalation into a nucleic acid lattice.

Finally, with the exception of poly[d(G-C)$_2$], the reduction in the *D* parameter of the red triplet state increases monotonically with the binding affinity of the drug to the polynucleotide targets (Figure 11), suggesting that these quantities are directly related. Reduction in the *D*-value is expected to increase with the extent of aromatic stacking interactions (Haenel & Schweitzer, 1988), further suggesting that the extent of aromatic stacking may play an important role in stabilizing echinomycin–DNA complexes. The fact that poly[d(G-C)$_2$], the only DNA investigated in this work that can readily assume a Z-conformation (Arnott et al., 1980), does not correlate with the other DNAs (the *D*-value increases upon drug binding, instead of decreasing) suggests that a structurally different complex with echinomycin may be formed.

Acknowledgments

We thank Dr. Matthew Suffness of the National Cancer Institute (Bethesda, MD), Drs. H. H. Peter and K. Scheibli of Ciba-Geigy AG (Basle, Switzerland), and Dr. Derek Hook and colleagues of Bristol-Myers Co. (Wallingford, CT) for their gifts of echinomycin. We also thank Dr. Michael J. Waring for helpful discussions concerning this work.

References

Alfredson, T. V., Maki, A. H., Adaskaveg, M. E., Excoffier, J.-L., & Waring, M. J. (1990) *J. Chromatogr. 507*, 277–292.

Arnott, S., Chandrasekaran, R., Birdsall, D. L., Leslie, A. G. W., & Ratcliff, R. L. (1980) *Nature 283*, 743–745.

Becker, H. K. (1988) *J. Chromatogr. 234*, 678–684.

Brenner, H. C., & Kolubayev, V. (1988) *J. Lumin. 39*, 251–257.

Bresloff, J. L.; & Crothers, D. M. (1981) *Biochemistry 20*, 3547–3553.

Casas-Finet, J. R., Khamis, M. I., Maki, A. H., Ruvolo, P. P., & Chase, J. W. (1987) *J. Biol. Chem. 262*, 8574–8583.

Casas-Finet, J. R., Jhon, N.-I., & Maki, A. H. (1988) *Biochemistry 27*, 1172–1178.

Chaires, J. B. (1983) *Biochemistry 22*, 4204–4211.

Cheung, H. T., Feeney, J., Roberts, G. C. K., Williams, D. H., Ughetto, G., & Waring, M. J. (1978) *J. Am. Chem. Soc. 100*, 46–54.

Chodkowska, A., Grabowska, A., & Herbich, J. (1977) *Chem. Phys. Lett. 51*, 365–369.

Clarke, R. H., Mitra, P., & Vinodgopal, K. (1982) *J. Chem. Phys. 77*, 5288–5297.

Fox, K. R., Wakelin, L. P. G., & Waring, M. J. (1981) *Biochemistry 20*, 5768–5779.

Gao, X., & Patel, D. J. (1988) *Biochemistry 27*, 1744–1751.

Gao, X., & Patel, D. J. (1989) *Q. Rev. Biophys. 22*, 93–138.

Gilbert, D. E., van der Marel, G. A., van Boom, J. H., & Feigon, J. (1989) *Proc. Natl. Acad. Sci. U.S.A. 86*, 3006–3010.

Gradl, G., & Friedrich, J. (1985) *Chem. Phys. Lett. 114*, 543–546.

Gradl, G., Friedrich, J., & Kohler, B. E. (1986) *J. Chem. Phys. 84*, 2079–2083.

Haenel, M. W., & Schweitzer, D. (1988) *Adv. Chem. Ser. 217*, 333–355.

Hayashi, H., Iwata, S., & Nagakura, S. (1969) *J. Chem. Phys. 50*, 993–1000.

Inoue, A., Nishi, N., Kinoshita, M., & Ebara, N. (1980) *Bull. Chem. Soc. Jpn. 53*, 2466–2467.

Iwata, S., Tanaka, J., & Nagakura, S. (1967) *J. Chem. Phys. 47*, 2203–2209.

Jones, M. B., Hollstein, U., & Allen, F. S. (1987) *Biopolymers 26*, 121–135.

Khamis, M. I., Casas-Finet, J. R., Maki, A. H., Murphy, J. B., & Chase, J. W. (1987a) *J. Biol. Chem. 262*, 10938–10945.

Khamis, M. I., Casas-Finet, J. R., Maki, A. H., Murphy, J. B., & Chase, J. W. (1987b) *FEBS Lett. 211*, 155–159.

Krebs, P., Sackmann, E., & Schwarz, J. (1971) *Chem. Phys. Lett. 8*, 417–420.

Kwiram, A. L., Ross, J. B. A., & Deranleau, D. A. (1978) *Chem. Phys. Lett. 54*, 506–509.

Lee, J. S., & Waring, M. J. (1978) *Biochem. J. 173*, 115–128.

Low, C. M. L., Drew, H. R., & Waring, M. J. (1984) *Nucleic Acids Res. 12*, 4865–4879.

Maki, A. H., & Co, T. (1976) *Biochemistry 15*, 1229–1235.

McGlynn, S. P., Azumi, T., & Kinoshita, M. (1969) in *Molecular Spectroscopy of the Triplet State*, pp 321–322, Prentice-Hall, Englewood Cliffs, NJ.

Mohwald, H., & Sackmann, E. (1974) *Chem. Phys. Lett. 26*, 509–513.

Sato, K., Shiratori, O., & Katagari, K. (1967) *J. Antibiot., Ser. A 20*, 270–281.

Schmidt, J., Antheunis, D. A., & van der Waals, J. H. (1971) *Mol. Phys. 22*, 1–17.

Schweitzer, D., Hausser, K. H., Taglieber, V., & Staab, H. A. (1976) *Chem. Phys. 14*, 183-187.
Sheldrick, G. M., Guy, J. J., Kennard, O., Rivera, V., & Waring, M. J. (1984) *J. Chem. Soc., Perkin Trans. 2 43*, 1601-1605.
Strum, J. (1982) *Biopolymers 21*, 1189-1206.
Suga, K., & Kinoshita, M. (1982) *Bull. Chem. Soc. Jpn. 55*, 1695-1704.
Tsao, D. H. H., Casas-Finet, J. R., Maki, A. H., & Chase, J. W. (1989) *Biophys. J. 55*, 927-936.
Ughetto, G., Wang, A. H.-J., Quigley, G. J., van der Marel, G. A., van Boom, J. H., & Rich, A. (1985) *Nucleic Acids Res. 13*, 2305-2323.
van der Waals, J. H., & de Groot, M. S. (1967) Magnetic Interactions Related to Phosphorescence, in *The Triplet State* (Zahlan, A. B., Ed.) pp 101-132, Cambridge University Press, Cambridge, England.
Van Dyke, M. M., & Dervan, P. B. (1984) *Science 225*, 1122-1127.
von Schütz, J. U., Zuclich, J., & Maki, A. H. (1974) *J. Am. Chem. Soc. 96*, 714-718.
Wakelin, L. P. G., & Waring, M. J. (1976) *Biochem. J. 157*, 721-740.
Wang, A. H.-J., Ughetto, G., Quigley, G. J., Hakoshima, T., van der Marel, G. A., van Boom, J. H., & Rich, A. (1984) *Science 225*, 1115-1121.
Ward, D. C., Reich, E., & Goldberg, I. H. (1965) *Science 149*, 1259-1264.
Waring, M. J., & Wakelin, L. P. G. (1974) *Nature 252*, 653-659.
Williamson, R. L., & Kwiram, A. L. (1988) *J. Chem. Phys. 88*, 6092-6106.
Wilson, W. D., Wang, Y.-H., Krishnamoorthy, C. R., & Smith, J. C. (1985) *Biochemistry 24*, 3991-3999.
Zang, L.-H., Maki, A. H., Murphy, J. B., & Chase, J. W. (1987) *Biophys. J. 52*, 867-872.
Zhou, N., James, T. L., & Shafer, R. H. (1989) *Biochemistry 28*, 5231-5239.

Histidine-40 of Ribonuclease T_1 Acts as Base Catalyst When the True Catalytic Base, Glutamic Acid-58, Is Replaced by Alanine†

Jan Steyaert,*,‡,§ Klaas Hallenga,‡ Lode Wyns,§ and Patrick Stanssens‡

Plant Genetic Systems NV, J. Plateaustraat 22, B-9000 Gent, Belgium, and Vrije Universiteit Brussel, Instituut Moleculaire Biologie, Paardestraat 65, B-1640 St-Genesius-Rode, Belgium

Received March 16, 1990; Revised Manuscript Received May 16, 1990

ABSTRACT: Mechanisms for the ribonuclease T_1 (RNase T_1; EC 3.1.27.3) catalyzed transesterification reaction generally include the proposal that Glu58 and His92 provide general base and general acid assistance, respectively [Heinemann, U., & Saenger, W. (1982) *Nature (London) 299*, 27-31]. This view was recently challenged by the observation that mutants substituted at position 58 retain high residual activity; a revised mechanism was proposed in which His40, and not Glu58, is engaged in catalysis as general base [Nishikawa, S., Morioka, H., Kim, H., Fuchimura, K., Tanaka, T., Uesugi, S., Hakoshima, T., Tomita, K., Ohtsuka, E., & Ikehara, M. (1987) *Biochemistry 26*, 8620-8624]. To clarify the functional roles of His40, Glu58, and His92, we analyzed the consequences of several amino acid substitutions (His40Ala, His40Lys, His40Asp, Glu58Ala, Glu58Gln, and His92Gln) on the kinetics of GpC transesterification. The dominant effect of all mutations is on k_{cat}, implicating His40, Glu58, and His92 in catalysis rather than in substrate binding. Plots of log (k_{cat}/K_m) vs pH for wild-type, His40Lys, and Glu58Ala RNase T_1, together with the NMR-determined pK_a values of the histidines of these enzymes, strongly support the view that Glu58-His92 acts as the base-acid couple. The curves also show that His40 is required in its protonated form for optimal activity of wild-type enzyme. We propose that the charged His40 participates in electrostatic stabilization of the transition state; the magnitude of the catalytic defect (a factor of 2000) from the His40 to Ala replacement suggests that electrostatic catalysis contributes considerably to the overall rate acceleration. For Glu58Ala RNase T_1, the pH dependence of the catalytic parameters suggests an altered mechanism in which His40 and His92 act as base and acid catalyst, respectively. The ability of His40 to adopt the function of general base must account for the significant activity remaining in Glu58-mutated enzymes.

Ribonuclease T_1 (RNase T_1, EC 3.1.27.3) from the fungus *Aspergillus oryzae* is the best known representative of a family of microbial ribonucleases sharing homology at both the sequence and structural level. The enzyme consists of a single polypeptide chain of 104 residues of known sequence and contains 2 disulfide bridges (Takahashi, 1971, 1985). The three-dimensional structure of RNase T_1, complexed with the competitive inhibitor guanosine 2'-phosphate (2'-GMP),[1] has been determined to 1.9-Å resolution by Heinemann and Saenger [1982; see also Arni et al. (1988) and Sugio et al.

† This work was supported by Plant Genetic Systems NV. J.S. is a Research Assistant of the Belgian National Fund for Scientific Research.
* Address correspondence to this author at the Vrije Universiteit Brussel.
‡ Plant Genetic Systems NV.
§ Vrije Universiteit Brussel.

[1] Abbreviations: barnase, *Bacillus amyloliquefaciens* ribonuclease; cGMP, guanosine cyclic 2',3'-phosphate; EDTA, ethylenediaminetetraacetic acid; 2'-GMP, guanosine 2'-phosphate; GpC, guanylyl(3'-5')cytidine; GpU, guanylyl(3'-5')uridine; IPTG, isopropyl β-D-thiogalactopyranoside; MES, 2-(*N*-morpholino)ethanesulfonic acid; rms, root mean square; Tris, tris(hydroxymethyl)aminomethane; UpU, uridylyl(3'-5')-uridine.

0006-2960/90/0429-9064$02.50/0